

Regularization fast multipole boundary element method for potential flow problems in 3D vortex method

Jie Zhai^{1,2}, Baoshan Zhu¹ & Shuliang Cao¹

¹*State Key Laboratory of Hydro Science Engineering, Tsinghua University, China*

²*Department of Thermal Engineering, Tsinghua University, China*

Abstract

The boundary element method (BEM) is one way for solving the normal flow boundary conditions (potential flow problem) and the pressure distribution in numerical simulation of the three-dimensional vortex method. Because the problem can be reduced from a three-dimensional integral to a two-dimensional integral by BEM, this method is acclaimed in this study. BEM in engineering calculations already has a good application, but with the increasing number of grid problems, the dense matrix generated in the conventional boundary element method (CBEM) is increasing sharply. The fast multipole method (FMM) is introduced to accelerate the computational efficiency and speed of BEM. The three-dimensional vortex method requires solving the velocity and the velocity gradient of potential flow by BEM, and then it will encounter strongly singular integrals. The semi-analytical integral regularization algorithm is applied for solving strongly singular integrals in this paper. The regularization fast multipole boundary element method (FMBEM) is applied to the potential problem of flow over a single sphere, and analyze the results to prove the reliability and efficiency of this method. The calculation parameters which are selected by comparing the influences of them in the single sphere problem are applied to the potential problem of flow over multi-spheres, and the results are analyzed.

Keywords: BEM, FMM, regularization algorithm, potential problem.



1 Introduction

For solving the normal flow boundary conditions in the three-dimensional vortex method, we need to work out the potential flow problem [1]. The potential flow problem can generally be described by a Laplace equation or Poisson equation. They can be solved by the finite difference method (FDM), finite element method (FEM) or boundary element method (BEM). Relatively, BEM has the following advantages: BEM is a semi-analytical method, so it has a higher accuracy; distributed discrete elements are only on the boundary of the physical model, so it can reduce to one-dimension, and the number of the unknowns [1, 5].

BEM in engineering calculations already has a good application, but with the increasing number of grid problems, the dense matrix generated in the conventional boundary element method (CBEM) is increasing sharply [1, 3, 4]. This matter not only increases the amount of calculation storage and reduces the computational efficiency, but it also cannot be solved in a general computer. Taking into account the fundamental solution in a BEM and N-body problem has the same mathematical model, so the fast multipole method (FMM) in an N-body problem is introduced to accelerate the computational efficiency and speed of BEM.

The three-dimensional vortex method requires solving the velocity and the velocity gradient of potential flow by BEM, and then it will encounter strongly singular integrals. The semi-analytical integral regularization algorithm is applied for solving strongly singular integrals in this paper.

The potential flow problem of flow over a sphere is a classical problem with an analytical solution, so the validity of the regularization fast multipole boundary element method (FMBEM) is checked by simulating this problem. The analyses of the numerical results prove the reliability and efficiency of the present method. The calculation parameters of FMM which are selected by comparing the influences of them in the single sphere problem are applied to the potential problem of flow around multi-spheres, and the numerical results are analyzed.

2 Fast multipole boundary element method

2.1 Conventional boundary element method

There are three ways to prove BEM: one is the weighted residual Galerkin method which translates the differential problem to an integral equation; a more rigorous method is solving the functional extremum in a variational method. Another more direct approach is starting from Green's theorem, which translates the domain integral to the boundary integral [5]. Here, the last method is used. In a potential flow problem, the potential field Φ in domain is described by the Poisson equation as below:

$$\Delta\Phi + f = 0 \quad (1)$$



where f is a known function in domain, and it assumes $f = 0$ here. And the boundary conditions (BCs) are:

$$\begin{aligned}\Phi &= \bar{\Phi} && \text{Dirichlet Boundary Condition} \\ q &= \frac{\partial \Phi}{\partial \mathbf{n}} = \bar{q} && \text{Neumann Boundary Condition}\end{aligned}$$

where q is the normal velocity on the surface. Here, we take the Neumann BC.

Eq. (1) can be reformulated in the following boundary integral form [4]:

$$\alpha(\mathbf{x})\Phi(\mathbf{x}) = \int_{\Gamma} \left(G(\mathbf{x}, \mathbf{y}) \frac{\partial \Phi(\mathbf{y})}{\partial \mathbf{n}_y} - \Phi(\mathbf{y}) F(\mathbf{x}, \mathbf{y}) \right) ds_y, \quad (2)$$

where $G = G(\mathbf{x}, \mathbf{y}) = 1/4\pi |\mathbf{x} - \mathbf{y}|$ is the three-dimensional Green function, $F(\mathbf{x}, \mathbf{y}) = \partial G(\mathbf{x}, \mathbf{y})/\partial \mathbf{n}_y$, is its normal flux, and coefficient $\alpha(\mathbf{x})$ is:

$$\alpha(\mathbf{x}) = \begin{cases} 1 & \mathbf{x} \in V-S \\ \frac{\theta(\mathbf{x})}{4\pi} & \mathbf{x} \in S \\ 0 & \mathbf{x} \in V^1-S \end{cases} \quad (3)$$

where $\theta(\mathbf{x})$ is a solid angle on the boundary surface, and $\alpha(\mathbf{x}) = 1/2$ if S is smooth around \mathbf{x} .

Once the boundary values of both Φ and q are known, we can calculate Φ everywhere in domain by Eq. (2), if needed. To solve the unknown boundary values, we let \mathbf{x} tend to the boundary S to obtain an equation from Eq. (2). Then we apply collocation techniques to discretize the integral in order to solve them numerically. The discrete boundary integral Eq. (2) yields:

$$\begin{aligned}\frac{1}{2} \Phi(\mathbf{x}^i) + \sum_{e=1}^{NE} \int_{\Gamma_e} F(\mathbf{x}^i, \mathbf{y}) \sum_{k=1}^K N^k(\xi) \Phi^k(\mathbf{x}^k) d\Gamma_e \\ = \sum_{e=1}^{NE} \int_{\Gamma_e} \bar{q} G(\mathbf{x}^i, \mathbf{y}) d\Gamma_e \quad i = 1, \dots, NP\end{aligned} \quad (4)$$

where K is the number of local nodes on each element, NE is the number of elements, NP is the number of nodes, N^k is the shape function. The two integrals which are singular at $r = 0$ of $O(r^{-1})$ and $O(r^{-2})$ can be solved by sub-element method [5] in Eq. (4).

The quadrilateral four-node elements are taken and the four shape functions are:



$$\begin{cases} N^1(\xi) = \frac{1}{4}(1 - \xi_1)(1 - \xi_2), & N^2(\xi) = \frac{1}{4}(1 + \xi_1)(1 - \xi_2) \\ N^3(\xi) = \frac{1}{4}(1 + \xi_1)(1 + \xi_2), & N^4(\xi) = \frac{1}{4}(1 - \xi_1)(1 + \xi_2) \end{cases} \quad (5)$$

Simplifying Eq. (4), we have:

$$[H]\{\Phi\} = B \quad (6)$$

The boundary potential values of nodes can be solved by linear Eq. (6).

To evaluate the potential velocity (the derivatives of the potential) in V , we take the derivative of Eq. (2) to obtain:

$$\alpha(x)u_k(x) = \int_{\Gamma} \frac{\partial G(x, y)}{\partial x_k} u_n(y) d\Gamma - \int_{\Gamma} \frac{\partial F(x, y)}{\partial x_k} \Phi(y) d\Gamma, k = 1, 2, 3 \quad (7)$$

2.2 Fast multipole method

The matrix H of Eq. (6) is dense matrix, so the amount of calculation operation increases $O(N^2)$ with the mesh number N . FMM, which is an acceleration method, is due to the fact that the Green's function can be expanded in the following form [3, 4, 7]:

$$\frac{1}{4\pi|\mathbf{x} - \mathbf{y}|} = \frac{1}{4\pi} \sum_{n=0}^{\infty} \sum_{m=-n}^n \bar{S}_{n,m}(\mathbf{x} - \mathbf{x}_c) R_{n,m}(\mathbf{y} - \mathbf{y}_c), |\mathbf{y} - \mathbf{y}_c| < |\mathbf{x} - \mathbf{y}_c| \quad (8)$$

where \mathbf{y}_c is the expansion center close to the field point \mathbf{y} . The two functions $R_{n,m}(\mathbf{x})$ and $S_{n,m}(\mathbf{x})$ are called solid harmonic functions, given by:

$$\begin{aligned} R_{n,m}(\mathbf{x}) &= \frac{1}{(n+m)!} P_n^{|m|}(\cos \alpha) e^{im\beta} \rho^n \\ S_{n,m}(\mathbf{x}) &= (n-m)! P_n^{|m|}(\cos \alpha) e^{im\beta} \frac{1}{\rho^{n+1}} \end{aligned}$$

where (ρ, α, β) are the coordinates of \mathbf{x} used in a spherical coordinate system. P_n^m is the associated Legendre function, and it is about the Legendre polynomials P_n of degree n .

By using Eq. (8), we can write the original integral as:

$$\int_{\Gamma} \frac{\partial G(\mathbf{x}^i, \mathbf{y})}{\partial \mathbf{n}_y} \Phi(\mathbf{y}) d\Gamma = \frac{1}{4\pi} \sum_{n=0}^{\infty} \sum_{m=-n}^n \bar{S}_{n,m}(\mathbf{x} - \mathbf{x}_c) M_{n,m}(\mathbf{y}_c) \quad (9)$$



$$\int_{\Gamma} u_n(\mathbf{y}) G(\mathbf{x}^i, \mathbf{y}) d\Gamma = \frac{1}{4\pi} \sum_{n=0}^{\infty} \sum_{m=-n}^n \bar{S}_{n,m}(\mathbf{x} - \mathbf{x}_c) \tilde{M}_{n,m}(\mathbf{y}_c) \quad (10)$$

where

$$M_{n,m}(\mathbf{y}_c) = \int_{\Gamma} \frac{\partial R_{n,m}(\mathbf{y} - \mathbf{y}_c)}{\partial \mathbf{n}_y} \Phi(\mathbf{y}) d\Gamma \quad (11)$$

$$\tilde{M}_{n,m} = \int_{\Gamma} u_n(\mathbf{y}) R_{n,m}(\mathbf{y} - \mathbf{y}_c) d\Gamma \quad (12)$$

When the multipole expansion center is moved from \mathbf{y}_c to $\mathbf{y}_{c'}$, we apply the following M2M translation:

$$M_{n,m}(\mathbf{y}_{c'}) = \sum_{n'=0}^n \sum_{m'=-n'}^{n'} R_{n',m'}(\mathbf{y}_c - \mathbf{y}_{c'}) M_{n-n',m-m'}(\mathbf{y}_c) \quad (13)$$

which is also valid for $\tilde{M}_{n,m}$.

The local expansion for Eq. (9) and Eq. (10) is given as:

$$\int_{\Gamma} \frac{\partial G(\mathbf{x}^i, \mathbf{y}(\xi))}{\partial \mathbf{n}_y} \sum_{k=1}^K \Phi^k N^k(\xi) d\Gamma_e = \frac{1}{4\pi} \frac{\partial}{\partial \mathbf{n}} \sum_{n=0}^{\infty} \sum_{m=-n}^n R_{n,m}(xy) L_{n,m}(Ox) \quad (14)$$

$$\int_{\Gamma} u_n(\mathbf{y}) G(\mathbf{x}^i, \mathbf{y}) d\Gamma = \frac{1}{4\pi} \sum_{n=0}^{\infty} \sum_{m=-n}^n \bar{S}_{n,m}(\mathbf{x} - \mathbf{x}_c) \tilde{L}_{n,m}(\mathbf{y}_c) \quad (15)$$

where

$$L_{n,m}(Ox) = \sum_{n'=0}^n \sum_{m'=-n'}^{n'} (-1)^n \bar{S}_{n+n',m+m'}(Ox) M_{n',m'}(Oy) \quad (16)$$

$$\tilde{L}_{n,m}(Ox) = \sum_{n'=0}^n \sum_{m'=-n'}^{n'} (-1)^n \bar{S}_{n+n',m+m'}(Ox) \tilde{M}_{n',m'}(Oy) \quad (17)$$

When the local expansion center is moved from \mathbf{x}_c to $\mathbf{x}_{c'}$, we apply the following L2L translation:

$$L_{n,m}(\mathbf{x}_{c'}) = \sum_{n'=0}^n \sum_{m'=-n'}^{n'} R_{n-n',m-m'}(\mathbf{x}_c - \mathbf{x}_{c'}) L_{n',m'}(\mathbf{x}_c) \quad (18)$$

which is also valid for $\tilde{L}_{n,m}$.

Eq. (6) can be rewritten as:

$$\sum_{i=1}^{NE} H_{ji} \Phi_i = \sum_q \sum_{i \in W_q} H_{ji} \Phi_i + \frac{1}{4\pi} \sum_{n=0}^{\infty} \sum_{m=-n}^n \bar{S}_{n,m}(Ox) M_{n,m}(Oy) \quad (19)$$

By Eq. (19), the estimated cost of FMBEM is reduced to $O(N)$. A hierarchical cell structure covering all of the boundary elements is used in this paper.



2.3 Regularization of the singular integral

From Eq. (7), the potential velocity equation can be reformulated as:

$$\alpha(\mathbf{x})u_k(\mathbf{x}) = \sum_{e=1}^{NE} \int_{\Gamma_e} \frac{1}{4\pi} \frac{r_k}{r^3} u_n d\Gamma_e - \sum_{e=1}^{NE} \int_{\Gamma_e} \frac{1}{4\pi} \left(\frac{n_k}{r^3} - \frac{3r_k r_n}{r^5} \right) \Phi(\mathbf{y}) d\Gamma_e \quad (20)$$

In Eq. (20), the integrals are singular at $r = 0$ of $O(r^{-3})$ and $O(r^{-5})$. When the point \mathcal{Y} is far from the boundary, Gaussian integral formula can be directly used to calculate the potential velocity. As \mathcal{Y} approaches the boundary, the sub-element method is invalid for this strongly singularity. We use the regularization algorithm to solve the integrals.

As shown in Figure 1, a quadrilateral isoparametric element 1234 is divided into two triangular sub-elements $\Delta 123$ and $\Delta 134$. A local orthonormal coordinate system $\xi\eta$ is assigned to $\Delta 123$. We assume the pedal of point \mathcal{Y} on the surface of element $\Delta 123$ is \mathbf{y}_0 , and a polar coordinate system $\rho\theta$ is set up with \mathbf{y}_0 as the origin and the initial position of the polar axis is parallel with $o\xi$ on the plane. Therefore we have:

$$\begin{cases} \xi = \xi_0 + \rho \cos \theta \\ \eta = \eta_0 + \rho \sin \theta \end{cases} \quad (21)$$

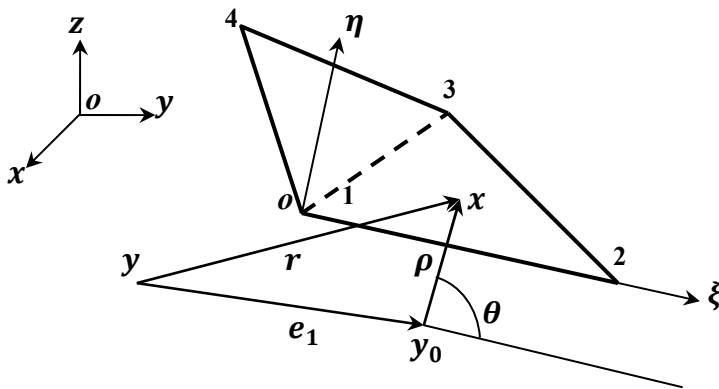


Figure 1: Boundary elements and three reference frame systems.

The shape function and geometrical coordinates for the element $\Delta 123$ are [8, 9]:

$$N_m(\xi, \eta) = \frac{1}{2A} (a_m + b_m \xi + c_m \eta) = \frac{1}{2A} \rho (b_m \cos \theta + c_m \sin \theta) + N_m(\xi_0, \eta_0) \quad (22a)$$

$$x_i = N_m(\xi, \eta)x_{mi} = \frac{1}{2A} \rho(b_m \cos \theta + c_m \sin \theta)x_{mi} + y_{oi} \quad i, m = 1, 2, 3 \quad (22b)$$

where A is area of $\Delta 123$, a_m, b_m, c_m are coefficient of (ξ_i, η_i) .

By equation (22b), we have:

$$r_i = x_i - y_i = \frac{1}{2A} \rho(b_m \cos \theta + c_m \sin \theta)x_{mi} + y_{oi} - y_i \quad (23)$$

$$r^2 = \rho^2 + e_1^2$$

where $e_1 = |\mathbf{y}_o - \mathbf{y}|$ is the smallest distance from the source point to Γ_e . We have the area equation of Γ_e :

$$d\Gamma = d\xi d\eta = \rho d\rho d\theta$$

Substituting the upper equations into Eq. (20), the integrals can be summarized as:

$$I_n = \int_{\Gamma_e} \frac{Q_n(\rho, \theta)}{r^n} \rho d\rho d\theta \quad n = 1, 3, 5, 7 \quad (24)$$

where $Q_n(\rho, \theta)$ is about $\rho, \cos \theta, \sin \theta$.

When e_1 is small, Gauss numerical integration fails. So small e_1 is the main reason causing the singular integral. First, Eq. (24) is taken integral by variable ρ , and we have:

$$K_n(\rho, \theta) = \int \frac{Q_n(\rho, \theta)}{r^n} \rho d\rho \quad n = 1, 3, 5, 7 \quad (25)$$

Subsection integral is repeatedly used to Eq. (25), we have a completely analytical formula for $K_n(\rho, \theta)$ can be obtained. Eq. (24) is calculated as:

$$I_n = \int_{\Gamma_e} K_n(\rho, \theta) \Big|_{\rho=\rho_1(\theta)}^{\rho=\rho_2(\theta)} d\theta \quad (27)$$

where $\rho_1(\theta)$ and $\rho_2(\theta)$ are decided by three lines 12, 23, 31. The strongly singular integrals of Eq. (20) are translating to a series of linear integrals to θ , and they can be calculated by the Gauss method.

3 Numerical results and analyses

3.1 Simulation of flow over a sphere

The potential flow problem of flow over a sphere is a classical problem with an analytical solution, so the validity of the regularization FMBEM is checked by simulating this problem.



For a sphere with radius a immersed in a uniform flow U , the potential in spherical coordinates of steady flow at the origin is:

$$\phi = U\left(r + \frac{1}{2} \frac{a^3}{r^2}\right) \cos \theta \tag{28}$$

and the potential velocity is

$$\begin{cases} u_r = U\left(1 - \frac{a^3}{r^3}\right) \cos \theta \\ u_\theta = -U\left(1 + \frac{1}{2} \frac{a^3}{r^2}\right) \sin \theta \\ u_\phi = 0 \end{cases} \tag{29}$$

Assume that $U = 1$ with \mathbf{x} direction and $a = 1$. To calculate numerical errors conveniently, we only consider the potential function of the dipole in Eq. (29) and Eq. (30). Figure 2 shows that the distribution of potential with $\alpha \in (0^\circ, 360^\circ)$ on the $\beta = \pi/2$ plane by three methods.

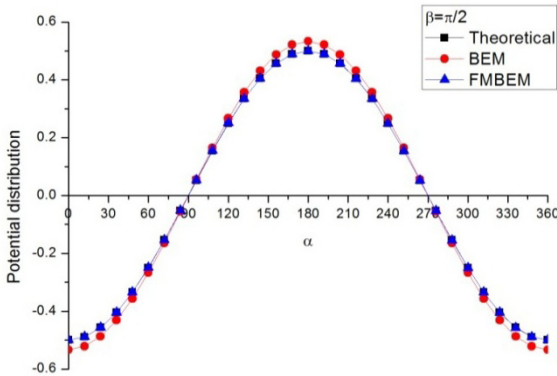


Figure 2: Distribution of potential vs. plane azimuth.

Table 1 shows that Φ standard error comparison between the regularization scheme and the Gaussian method. d is the distance from source point to the sphere surface. For convenient analysis, we define that d/a is the proximity. It can be seen that $d/a = 0.1$ is a critical point. When $d/a > 0.1$, the accuracy of the two methods are close. As $d/a < 0.1$ the accuracy of the Gaussian method deteriorates significantly. As $d/a < 0.001$ the Gaussian method is invalid, but

the regularization technique can calculate the potential with high accuracy ($O(10^{-5})$). Figure 3 shows that the potential velocity field on the $z = 0$ plane.

Table 1: Φ error comparison between regularization scheme and Gaussian method.

Distance d	Gauss Method (%)	Regularization Algorithm (%)
1.00	1.01	1.01
4.64E-1	1.01	1.01
2.15E-1	1.02	1.02
1.00E-1	1.87	1.87
4.64E-2	36.52	2.14
2.15E-2	653.95	0.31
1.00E-2	4941.23	1.87
2.15E-3	29085.51	1.28
1.00E-3	36452.07	1.83
4.64E-4		2.51
2.15E-4		3.66
1.00E-4		3.50
1.00E-5		5.21
1.00E-6		1.14

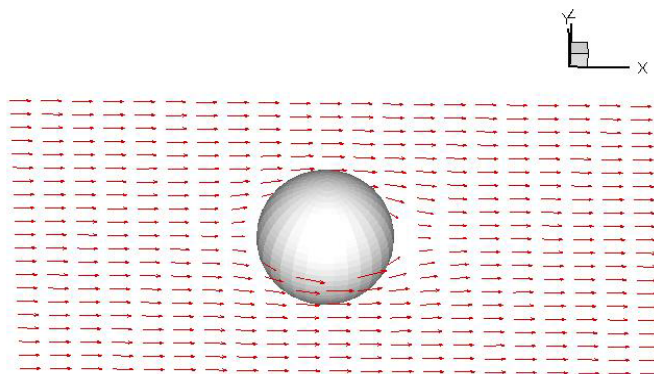


Figure 3: Potential velocity field on $z=0$ plane.

3.2 Analyses of FMBEM

In this part, we analyze the effect of FMM parameters and choose the proper parameters for complex problems. Figure 4 shows the CPU time comparison between BEM and FMBEM. It can see that FMBEM can accelerate computing speed significantly when the mesh number is great.

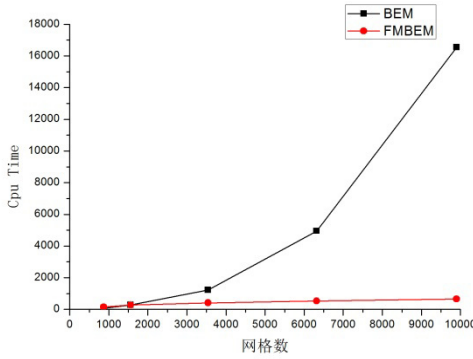


Figure 4: CPU time comparison by BEM and FMBEM.

p is the expansion coefficient of FMM. Figure 5 is the analysis of the effect of p . The dash lines are a series of potential root-mean-square errors vs. different p from 5 to 40. The solid lines are a series of CPU time vs. different p . CPU time increases exponentially with the increase of p . The errors decreases with the increase of p . Considering the time and accuracy, we choose $p = 15 \sim 30$.

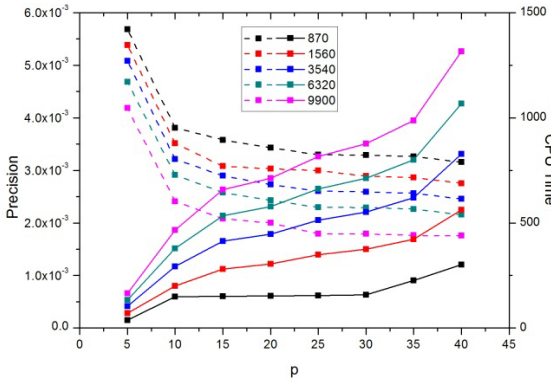


Figure 5: Analysis of the effect of FMM expansion coefficient p .

s is the max number elements in one cell. Figure 6 is the analysis of the effect of s . The dash lines are a series of potential root-mean-square errors vs. different s from 5 to 40. The solid lines are a series of CPU time vs. different s . CPU time increases exponentially with the increase of s . The errors decreases with the increase of s . $s = 20$ is an inflection point for root-mean-square errors. Considering the time and accuracy, we choose $s = 10 \sim 20$.

3.3 Multi-spheres results

The present method is applied to flow over multi-spheres potential problems. The FMM parameters are chosen by $p = 20$ and $s = 15$. The numerical results of two spheres and four spheres are shown below. Figure 7 is the comparisons of



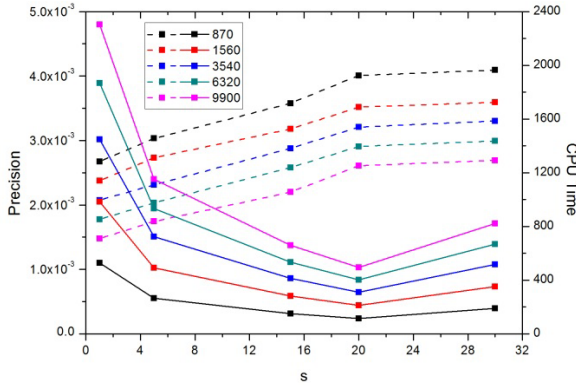


Figure 6: Analysis of the effect of FMM element coefficient s .

CPU time and root-mean-square errors between BEM and FMBEM of potential on boundary surface with different mesh numbers. It can see that FMBEM can accelerate computing speed significantly when the mesh number is great. And the potential of BEM and FMBEM is close to $O(10^{-3})$. Figure 8 shows that the potential velocity field of two spheres and four spheres problems on $z = 0$ plane.

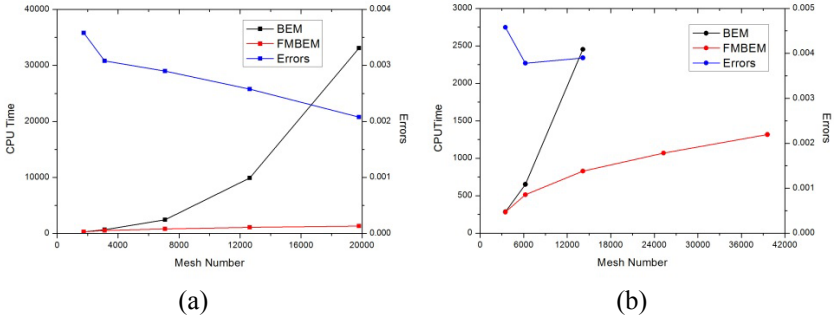


Figure 7: The comparison of CPU time and errors by BEM and FMBEM.

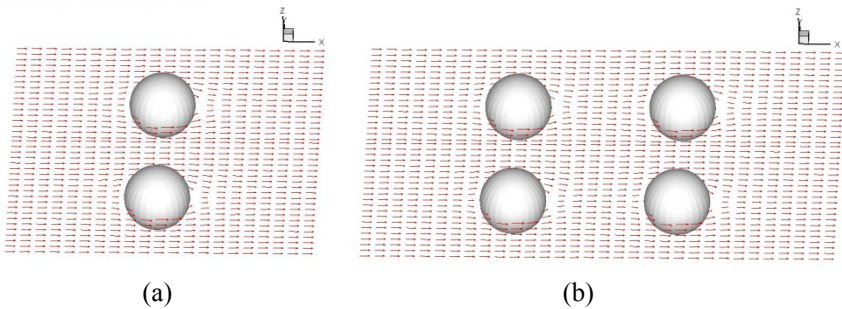


Figure 8: Potential velocity field of multi-spheres on $z = 0$ plane.

4 Conclusion

In this paper, we propose a more efficient comprehensive numerical hybrid method, the regularization FMBEM, for the potential flow problem in the three-dimensional vortex method. This paper gives a theoretical derivation of the numerical method, and this method can accelerate the computing time of conventional BEM, and calculate the strongly singular integrals.

The present method is applied to the potential flow over sphere. Through the numerical results, we verify the effectiveness of the regularization FMBEM. Analyze the effect of FMBEM parameters to CPU time and accuracy, and choose the proper parameters for the potential flow over complex shapes, such as, the potential flow over two spheres and four spheres.

References

- [1] Gharakhani A, Ghoniem A F. BEM solution of the 3D internal Neumann problem and a regularized formulation for the potential velocity gradients. *International Journal for Numerical Methods in Fluids*, 1998, 24(1): 81–100.
- [2] Liu Y, Rudolph T. Some identities for fundamental solutions and their applications to weakly-singular boundary element formulations. *Engineering Analysis with Boundary Elements*, 1991, 8(6): 301–311.
- [3] Liu Y J, Nishimura N. The fast multipole boundary element method for potential problems: A tutorial. *Engineering Analysis with Boundary Elements*, 2006, 30(5): 371–381.
- [4] Liu Y. Fast multipole boundary element method: theory and applications in engineering [M]. Cambridge University Press, 2009.
- [5] Cai Ruiying, et al. Boundary element method theory and application (in Chinese) [M]. Jiangsu Science and Technology Press, 1996.
- [6] Mukherjee S. CPV and HFP integrals and their applications in the boundary element method. *International Journal of Solids and Structures*, 2000, 37(45): 6623–6634.
- [7] Greengard L, Rokhlin V. A new version of the fast multipole method for the Laplace equation in three dimensions. *Acta numerica*, 1997, 6(1): 229–269.
- [8] Zhou Huan-lin, Niu Zhong-rong, Wang Xiu-xi, Regularization of Nearly Singular Integrals in the Boundary Element Method for 3D Potential Problems. *Chinese Journal of Computational Physics*, 2005, 11, 22(6): 6.
- [9] Zhou Huan-lin, Niu Zhong-rong, Wang Xiu-xi, Regularization of Nearly Singular Integrals in the Boundary Element Method of Potential Problems. *Applied Mathematics and Mechanics*, 2003, 24(010): 1069–1074.
- [10] Yasuda Y, Higuchi K, Oshima T, et al. Efficient technique in low-frequency fast multipole boundary element method for plane-symmetric acoustic problems. *Engineering Analysis with Boundary Elements*, 2012, 36(10): 1493–1501.

